Supplementary information

A hydrogel-based Janus passive cooling material with both high solar reflectance and remarkable self-cleaning capability

Qingxi Xin[a], Kefan Chen[b], Yutong Chen[a], Liwu Zhou[a], Dengwei Jing*

[a] State Key Laboratory of Multiphase Flow in Power Engineering & International Research Center for Renewable Energy, School of Energy and Power Engineering, Xi'an Jiaotong University, Xi'an, Shaanxi 710049, China

[b]State Grid Chongqing Electric Power Company, State Grid Chongqing Electric Power Research Institute, Chongqing, 404100, China

*Corresponding author: Tel.: +86-29-82668769, Email: dwjing@mail.xjtu.edu.cn

1.Mass content of ZnO nanoparticles

$$Mass\ fraction = \frac{m_{ZnO}}{m_{AM} + m_{alginate}} \#(1)$$

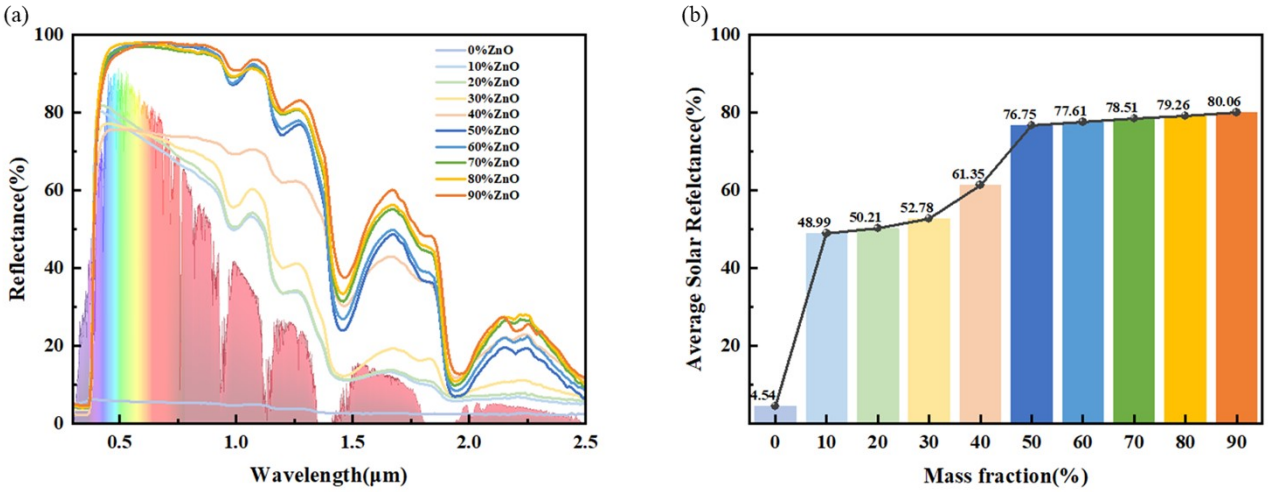

Figure S1: (a) Spectral reflectance of the hydrogel with different particles mass fraction; (b) Average solar reflectance of the hydrogel with different particles mass fraction.

2.Wet-dry cycles test

As illustrated in Figure S2, a 30×30 mm hydrogel sample was immersed in deionized water for one hour and then exposed to 1000 $W \cdot m^{-2}$ of xenon lamp radiation for one hour, repeating this cycle ten times. After immersion in deionized water for 1 hour, the hydrogel exhibited a 61% increase in mass, and its side length expanded from 30 mm to approximately 35 mm, as shown in Figure

S2(b).After the ten cycles, the average solar reflectance of the hydrogel decreased slightly from 80.06% to 77.71%, while the water contact angle changed from 133° to 130°, as shown in Figure S2(c). The hydrogel maintained a high solar reflectance and its contact angle decreased only slightly, demonstrating excellent durability and stability under repeated wet-dry and irradiation conditions.

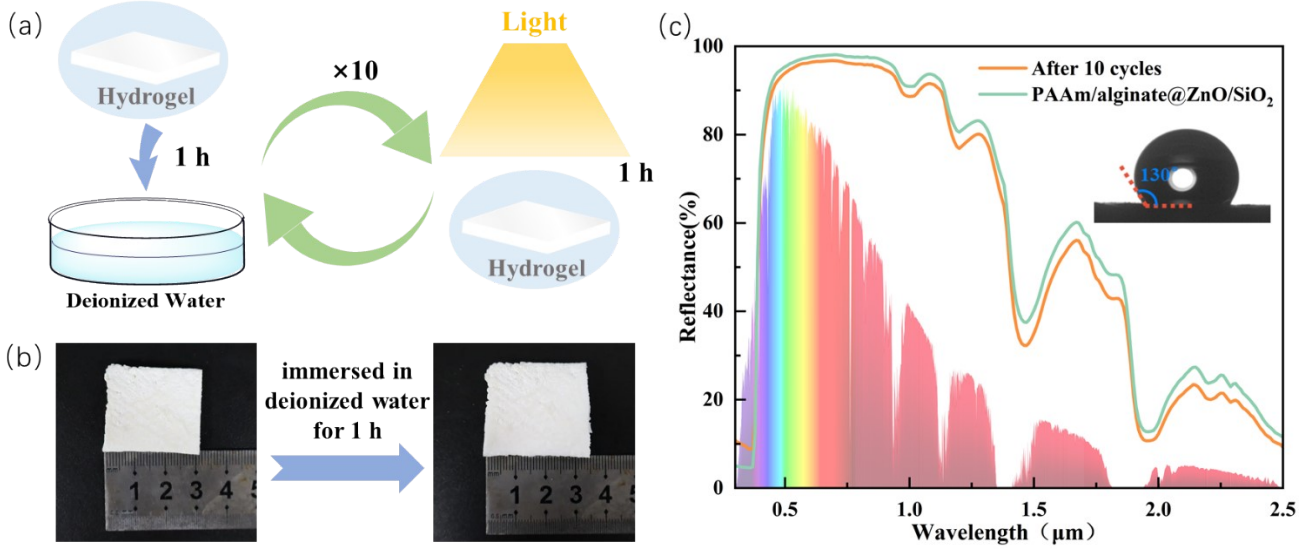

Figure S2: (a) Schematic of the Experimental Process. (b) Photographs showing the hydrogel before and after immersion in deionized water for 1 hour. (c) Comparison of the spectral reflectance of the hydrogel before and after ten wet–dry cycles, along with water contact angle photographs taken after the tenth cycle.

3.Outdoor test equipment

The photograph of the inside of the measuring box is shown in Figure S1. Samples are placed on the top of the chambers, and four thermocouples (KPS-TT-K-30-SLE, Xinghua Suma Electric Instruments Co., Ltd.) are attached on the bottom of samples in the chambers to record the real-time temperatures. And a temperature transducer (KWL-RDK-08A, Zhengzhou Keweilai Electronic Technology Co., Ltd.) is employed to convert the temperature signals into RS485 signals. A temperature and humidity sensor (SOBEST SM7820B, Shanghai Sonbest Industrial Co., Ltd.) is used to acquire the environmental temperature and relative humidity outside the testing chamber. The solar irradiation of incident sunlight is measured by a pyranometer (PR-300AL-RA-N01, Shandong Environmental Monitoring Co., Ltd.), and are converted from 4-20 mA to 485 signals by a signal conversion module (ZTS-3000-I20-4, Zhaotaisheng Technology Co., Ltd.). Wind speed is obtained from a wind speed sensor (RS-FSJT-N01, Shandong Renke Control technology Co., Ltd.). Finally, all the signals are connected to a 4G DTU (IOTROUTER ZHC4013, Chengdu Zongheng Intelligent

Control Technology Co., Ltd.). All the devices are powered by a 12V lithium battery (601-1, Shenzhen Yisenneng Technology Co., Ltd.).

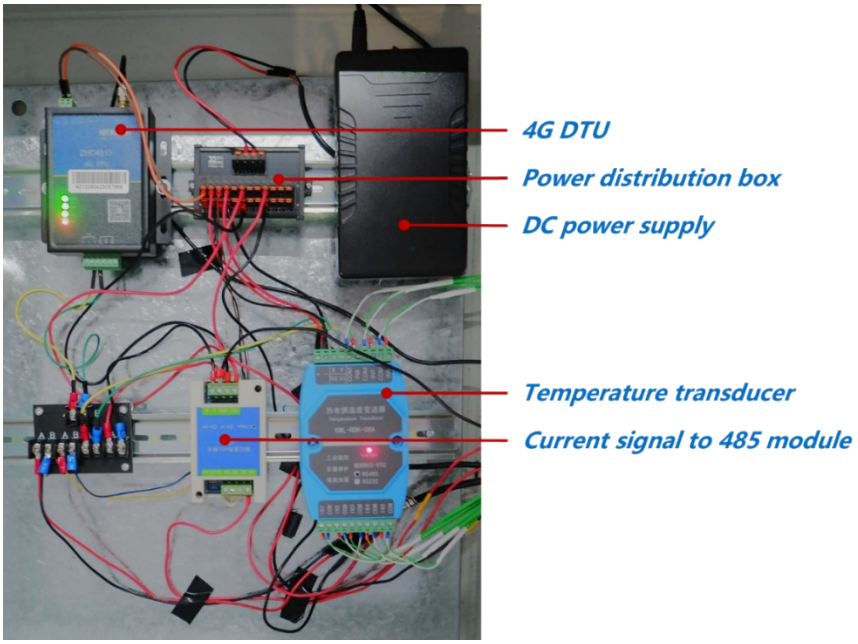

Figure S3. Photograph of the inside of the measuring box

4. Comparison of passive cooling performance

We compared the passive cooling performance of the designed PAAm/alginate@ZnO/SiO_2 hydrogel with some published hydrogel-based passive cooling material in Table S1.

Table S1. Recent impressive bilayer passive cooling structures

Bilayer Materials						
Upper layer	Lower layer	*solar*	LWIR	Solar intensity（$W \cdot m^{-2}$)	ΔT(°C)	Ref.
P(VdF-HFP)	PAAm-Li	0.960	0.960	~800	~7	1
PDMS	PAAm-$CaCl_2$	0.930	0.952	874.4	10.4	2
PTFE	PAAm/alginate-$CaCl_2$	/	/	/	6.4	3
Cellulose acetate	PVA-$CaCl_2$	0.950	0.940	~980	10	4
P(VdF-HFP)	PAAm/alginate-$CaCl_2$	0.916	0.900	706.3 378.0	15.4 6.3	5
P(VdF-HFP)	PVA/PA-LiCl	~0.96	~0.97	~800	~6	6
Monolayer Materials						

Material	Solar intensity（$W \cdot m^{-2}$)	ΔT(℃)	Ref.
PAAm/alginate@ZnO/SiO_2	709.3 575.8	27.4 18.4	This work
NPs/NADES@PAAm/PVA	~720	6.2	[7]
PAM-CNT-$CaCl_2$	1000	10	[8]
PAM-CB-LiCl	1000	9.9	[9]

Reference

1. C. Z. Feng, P. H. Yang, H. D. Liu, M. R. Mao, Y. P. Liu, T. Xue, J. Fu, T. Cheng, X. J. Hu, H. J. Fan and K. Liu, *Nano Energy*, 2021, **85**.
2. Z. Hu, Y. Qiu, J. Zhou and Q. Li, *Small Science*, 2024, **4**, 2300237.
3. Z. Li, T. Ma, F. Ji, H. Shan, Y. Dai and R. Wang, *ACS Energy Letters*, 2023, **8**, 1921-1928.
4. J. Li, X. Wang, D. Liang, N. Xu, B. Zhu, W. Li, P. Yao, Y. Jiang, X. Min, Z. Huang, S. Zhu, S. Fan and J. Zhu, *Science Advances*, 2022, **8**, eabq0411.
5. Q. X. Xin, B. C. Ma, J. Y. Ru, Y. Zhou and D. W. Jing, *Advanced Energy Materials*, 2025, **15**.
6. C. Guo, H. Tang, P. Wang, Q. Xu, H. Pan, X. Zhao, F. Fan, T. Li and D. Zhao, *Nature Communications*, 2024, **15**, 6100.
7. L. Xu, D.-W. Sun, Y. Tian, T. Fan and Z. Zhu, *Chemical Engineering Journal*, 2023, **457**, 141231.
8. R. Li, Y. Shi, M. Wu, S. Hong and P. Wang, *Nature Sustainability*, 2020, **3**, 636-643.
9. Y. Liu, Z. Liu, Z. Wang, W. Sun and F. Kong, *Applied Thermal Engineering*, 2024, **240**, 122185.